THE AMERICAN SOCIETY OF MECHANICAL ENGINEERS
345 E. 47th St., New York, N.Y. 10017

94-GT-334

EVALUATION AND PREDICTION OF BLADE-PASSING FREQUENCY NOISE GENERATED BY A CENTRIFUGAL BLOWER

Yutaka Ohta , Eisuke Outa , and Kiyohiro Tajima
Department of Mechanical Engineering
Waseda University
Tokyo , Japan

ABSTRACT

The blade-passing frequency noise, abbreviated to BPF noise, of low specific speed centrifugal blower is analyzed by separating the frequency-response of the transmission passage and the intensity of the noise source. Frequency-response has previously been evaluated by the authors using a one-dimensional linear wave model, and the results have agreed well with the experimental response in a practical range of the blower speed. In the present study, the intensity of the noise source is estimated by introducing the quasi-steady model of the blade wake impingement on the scroll surface. The effective location of the noise source is determined by analyzing the cross-correlation between measured data of the blower suction noise and pressure fluctuation on the scroll surface. Then, the surface density distribution of a dipole noise source is determined from pressure fluctuation expressed in terms of quasi-steady dynamic pressure of the traveling blade wake. Finally, the free-field noise level is predicted by integrating the density spectrum of the noise source over the effective source area. The sound pressure level of the blower suction noise is easily predicted by multiplying the free-field noise level by the frequency-response characteristics of the noise transmission passage.

NOMENCLATURE

A_2	$\pi D_2{}^2/4$ (m^2)
a	Speed of sound (m/s)
Csa	Cross-correlation function between Ps and Pa
Css	Cross-correlation function between Ps_1 and Ps_2
D	Surface density spectrum of noise source
D_2	External diameter of impeller (460 mm)
F_M	Frequency-distribution function in Eq.(1)
f	Frequency (Hz)
G_0	Frequency-response function in Eq.(1)
He	Helmholtz number, $He = f D_2/a$
K_D	Machine constant in Eq.(1)
k	Wave number, $k = 2\pi f/a$
Li	Inlet duct length (mm)
N	Blower rotational speed (rpm)
n_b	Number of impeller blade-to-blade passages
Pa	Sound pressure with ideal transmission (Pa)
Pam	Sound pressure radiated from blower (Pa)
P_0	Reference pressure, $P_0=2\times10^{-5}$ Pa
Ps	Pressure fluctuation on the scroll surface (Pa)
ΔP	Amplitude of surface pressure fluctuation (Pa)
Ri	Distance from blade trailing edge (mm)
Rsa	Cross-spectral density function between Ps and Pa
$Rsam$	Cross-spectral density function between Ps and Pam
r	Distance between noise source and measuring location (mm)
r_0	Radius of the scroll cut off (mm)
Δr_c	Clearance between impeller and scroll cut off (mm)
S	Frequency-correction function in Eq.(1)
Sa	Power spectral density of Pa
Sam	Power spectral density of Pam
S_b	Cross-sectional area of a blade-to-blade passage
Si	Clearance between impeller and inlet duct (mm)
St_D	Strouhal number, (St_D=1:1st BPF, St_D=2:2nd BPF)
S_2	Cross-sectional area of inlet duct
U_2	Impeller tip speed (m/s)
Vc	Freestream velocity (Absolute flame) (m/s)
ΔV	Amplitude of blade wake (Absolute flame) (m/s)
ΔW	Duration of blade wake (ms)
x	Position vector of noise measuring location
y	Position vector of noise source
Z	Number of impeller blades
α	Impingement angle (deg)
ρ	Density (kg/m^3)
σ	Non-dimensional specific speed, $\sigma = \phi^{1/2}/\psi^{3/4}$

Presented at the International Gas Turbine and Aeroengine Congress and Exposition
The Hague, Netherlands — June 13–16, 1994
This paper has been accepted for publication in the Transactions of the ASME
Discussion of it will be accepted at ASME Headquarters until September 30, 1994

ϕ	Flow coefficient
ψ	Pressure coefficient
θ	Angle between surface normal and direction of noise radiation (deg)
ω	Angular velocity (rad/s)

Subscripts

m	Effect of noise transmission passage
opt	Maximum-efficiency operation

Superscripts

—	Time average
*	Scroll surface

INTRODUCTION

In case of low specific speed centrifugal fans or blowers, the BPF noise could dominate the overall noise level, if sufficient care is not taken. Therefore, many of the blower noise investigations such as, Weidemann's (1971), Neise's (1975, 1976), Suzuki et al.'s (1977) and Bommes's (1982) have been made with special attentions to the prediction of the BPF components. However, the complete understandings have not yet been established, since the BPF components depend not only on the source strength but also on the frequency-response characteristics of the noise transmission passage.

In the present study, the experimental evaluation of both contribution was made by sweeping the blower rotational speed with a precise resolution, and the similarity rule developed by Neise (1975, 1976) and Bommes (1982) was utilized for data reduction. The influence of several blower design parameters was discussed for each of the similarity terms constituting the rule.

The frequency-response of the noise transmission passage has been described by introducing a one-dimensional linear wave model, in which the key parameter is the number of blade-to-blade passages selectively determined by the noise wavelength. Application of the model, allowing the selection of the inlet duct length, the blower rotational speed and the number of blades, facilitates reducing the noise level transmitted to the blower exterior without any effect on blower performance (Ohta et al., 1987).

One of the most comprehensive method to define the noise source extent may be the correlation analysis. Curle (1955), Siddon (1973), Akishita et al. (1978), and Maruta and Kotake (1979a, 1979b) have been made to analyze the aerodynamic noise radiated from flat plates or aerofoils immersed in steady flow. The authors intend to utilize the correlation analysis based on Lighthill's (1952) dipole theory for the BPF component radiated from a centrifugal blower. The extent of the effective source region was determined by measuring the cross-correlation between the data of the acoustic pressure and the pressure fluctuation on the scroll surface (Ohta et al., 1991). As usually expected, the location of the effective source was restricted to the vicinity of the scroll cut off, irrespective of the cut off geometries. The free-field noise characteristics were then obtained by integrating the surface density spectrum of the dipole source over the effective extent on the scroll surface. A quasi-steady model of blade wake impingement was applied to express surface pressure fluctuation, and dipole strength was calculated by taking the cross-correlation between the pressures measured at two different locations on the scroll surface. The key parameters were the extent of the noise source and the velocity profile of the blade wake diffusing towards the cut off surface.

The next stage of interest is thus focused on an increase of the BPF noise level in accordance with the decrease of flow rate from the maximum-efficiency operation. A preliminary discussion is made tentatively to predict the off-designed noise level by utilizing the present model.

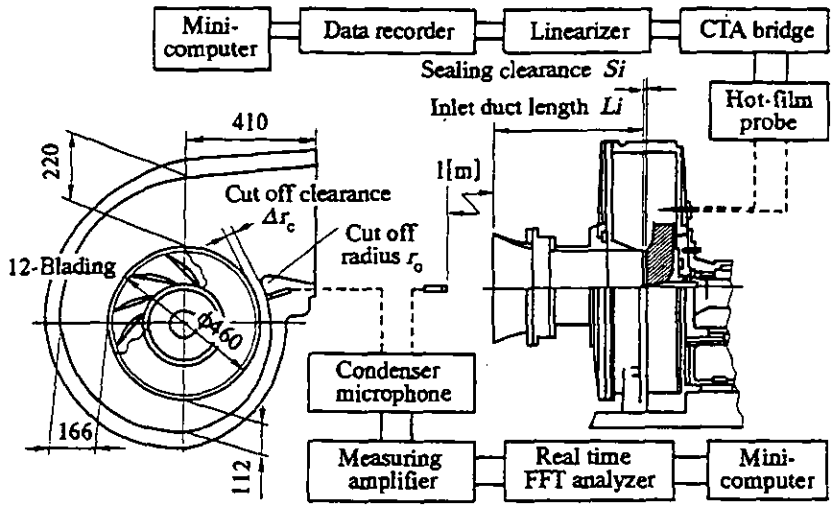

FIG. 1 EXPERIMENTAL APPARATUS AND MEASURING SYSTEMS.

TABLE 1 DESIGN PERFORMANCE OF TESTED BLOWER.

Rotational speed	N	3000	rpm
Volume flow rate	Q	50.0	m^3/min
Total pressure rise	Pt	300	mmAq
Specific speed	Ns	42.4	rpm,m^3/s, m
Gas horsepower	Lat	3.59	kW

TABLE 2 IMPELLER DIMENSIONS.

Number of blades	Z	12
Inlet diameter	D_1	260 mm
Outlet diameter	D_2	460 mm
Blade shape		NACA-65

EXPERIMENTAL FACILITY

Tested Centrifugal Blower

The centrifugal blower and the data acquisition system are schematically shown in Fig.1. The blower rotational speed is swept every 50 rpm within the range between 1000 and 4500 rpm. The operation point is set by a butterfly valve installed at the end of the outlet duct of 16.7 m length. The blower volume flow rate is measured using an orifice flow meter at the outlet duct. Impeller dimensions and specifications of blower performance are listed in Tables 1 and 2.

The blower external noise is obtained by the sound pressure measurement at the location 1 m apart from the inlet bellmouth. As recognized in previous researches, the cut off clearance Δr_c which is the distance between the impeller periphery and the scroll cut off, as well as the radius of the cut off r_0, give direct influence on the BPF components. In the present study, therefore, three types of cut off geometries are analyzed, i.e. (Δr_c=12 mm, r_0=12 mm), (Δr_c=32 mm, r_0=12 mm) and (Δr_c=12 mm, r_0=1.5 mm).

Measurement Methode

The blower suction noise *Pam* is measured using a B&K 4133 microphone at a location 1 m apart from the inlet bellmouth. The pressure fluctuation data *Ps* are acquired over the whole surface of the casing wall. Since the vicinity of the scroll cut off is thought as the most effective area of the noise source, the precise distribution of the fluctuation is carefully recorded. In the measurement, 1/8-inch precision microphones of B&K 4138 are used mounting flush to the scroll surface.

Instantaneous flow velocity and angle of the impeller discharge are also measured every 50 rpm by a constant temperature hot-film anemometer. An X-type nickel-coated quartz-fiber of DANTEC 55R52 is used. The probe is mounted to a rotatable and axially traversable support, and is inserted from the rear casing wall. The X-fibers are placed in the impeller meridional plane in such a manner that the velocity vector lies in the probe plane. Data sampling period is 2×10^5 times per second, and each of the velocity and the flow angle waveforms is averaged 120 times with a pulse trigger train generated every one revolution of the impeller.

SIMILARITY RULE OF BLOWER NOISE

The present analyses and discussion are based on a similarity rule of the inlet acoustic pressure *Pam* at the fundamental and the 2nd harmonic frequency of the BPF components, which is expressed as

$$\left(\frac{Pam}{P_0}\right)^2 = \underbrace{k_0 \frac{A_2}{4\pi}\left(\frac{\pi}{Z}\right)^{\gamma}}_{K_D} \underbrace{\frac{F_0(St_D)}{St_D{}^{\gamma}}}_{F_M} \underbrace{G_0(He)\,He^{\gamma}}_{G_M} \underbrace{S(\sigma, St_D : He)}_{S_M}. \quad (1)$$

In the expression, blower rotational speed is normalized by Helmholtz number *He* and the harmonics of the BPF components are denoted by Strouhal number St_D. The power of the blower inlet noise is expressed as a product of the

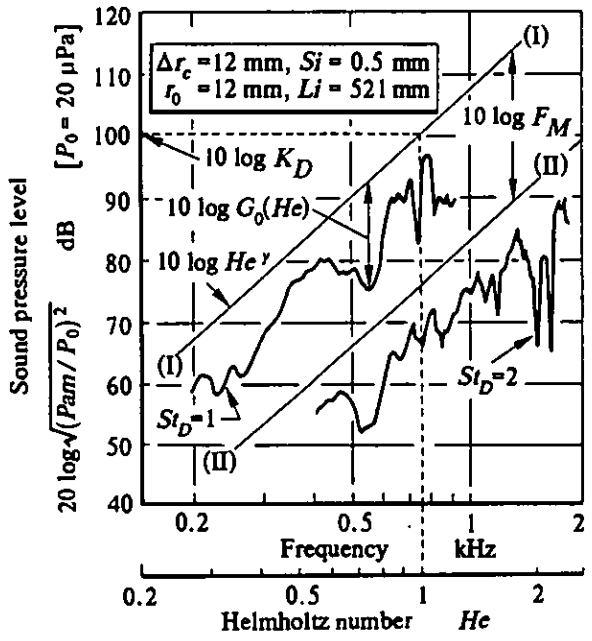

FIG. 2 LOCI OF BPF COMPONENTS VERSUS BLOWER ROTATIONAL SPEED.

following four terms:

(1) K_D: A machine constant representing the r.m.s. level of the free-field characteristics of the 1st BPF component. The value is indicated in Fig.2 as the ordinate of the ideal free-field characteristic (I)-(I) at a standard frequency of *He* =1. This term takes a constant value particular to each machine, and is related to the so-called specific sound power level.

(2) F_M: Amplitude ratios of the higher harmonics to the 1st BPF component. For the 2nd harmonics, i.e. St_D=2, the value is denoted in Fig.2 as a level shift between free-field characteristics (I)-(I) and (II)-(II) of the fundamental and the 2nd harmonics. This term is evaluated at the frequency but not at the operational speed of the impeller. For the tested blower, the 3rd and the higher components are not taken into account, since they slightly exceed the broad-band noise level.

(3) G_M : Frequency-dependent product of functions $G_0(He)$ and He^{γ}. The function $G_0(He)$ describes the frequency-response of the noise transmission passage. The second function He^{γ} represents the usual power-law relationship of noise increase versus convection velocity, and in the case of a dipole source γ can be assumed as 6.

(4) S_M : A supplementary correction function due to the harmonics of BPF and the deviation σ from the maximum-efficiency operation.

The frequency-response function $G_0(He)$ is overlaid in narrow shaded zones in Fig.3 for wide varieties of cut off geometries. By introducing a one-dimensional linear wave model, $G_0(He)$ has been evaluated as shown by thick and broken lines in Fig.3. The results agree well with the experimental data, and may be applied for practical use. The effective number n_b of the blade passage where the generated

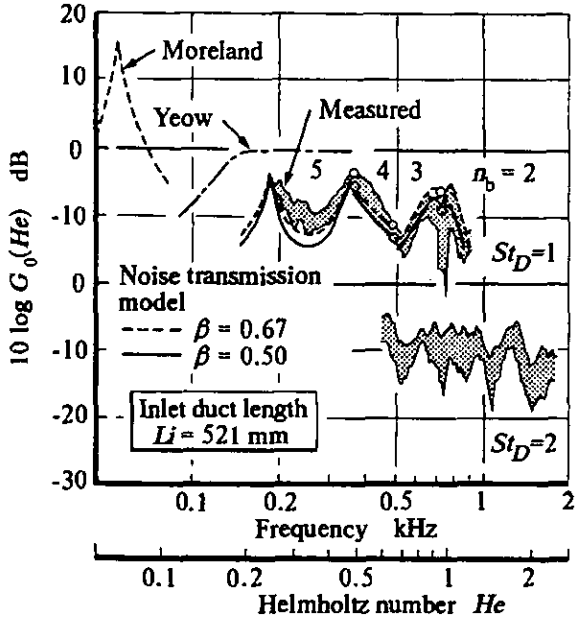

FIG. 3 FREQUENCY-RESPONSE OF THE TRANSMISSION PASSAGE DETERMINED BY EXPERIMENTS AND BY A WAVE MODEL.

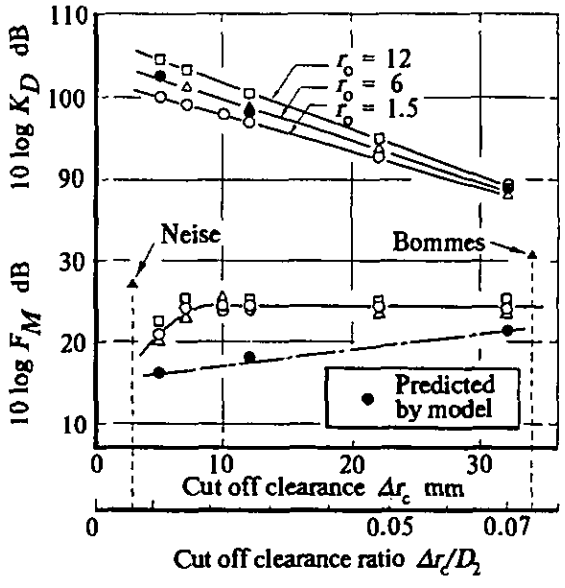

FIG. 4 SOURCE STRENGTH TERMS OF THE SIMILARITY RULE DETERMINED BY EXPERIMENTS AND PREDICTED BY A QUASI-STEADY FLOW MODEL.

noise transmits from the cut off is selected between 2 and 5, depending on the frequency range. This selection of the effective number n_b by the noise wavelength is considered to characterize the noise transmission mechanism of the blower system (Ohta et al., 1987). The results of lumped impedance models such as, Moreland's (1974) and Yeow's (1974a, 1974b) describe considerably lower frequency phenomena than that of the industrial noise concerned.

The source strength terms K_D and F_M are found to indicate a simple relationship to the distance between the cut off and the impeller as shown by open circles in Fig.4. However, quantitative evaluation of these terms requires information about the velocity profile of the impeller discharge flow, the diffusing process of the blade wake, and conversion mechanism to the pressure fluctuation on the scroll surface. Extent of the effective noise source should also be determined for the analysis.

CHARACTERISTICS OF THE NOISE SOURCE

Procedure of Source Noise Prediction

The procedure to predict the source strength terms K_D and F_M in Eq.(1) has the three steps discussed below. It is necessary in the procedure to determine the velocity distribution of the impeller discharge and the extent of the noise source by experimental measurements.

Step 1: The distribution of the BPF noise source on the scroll surface is determined using a correlation analysis between the acoustic pressure *Pam* at the inlet and the pressure fluctuation *Ps* on the whole surface of the casing wall, referred to as *Rsam* in Fig.5. In the analysis, dipole noise is assumed. Then, the extent of the effective source distributed on the scroll surface is obtained.

Step 2: The free-field characteristic of the BPF noise is obtained by integrating distributed pressure fluctuations in the source extent on the scroll surface; see *Rss* in Fig.6. The surface density spectrum of the noise source is calculated by taking a product of power spectral density of the pressure fluctuation and the correlation area which is determined by integrating the cross-spectral density of the pressure fluctuation data. Then, integration of the surface density spectrum over the effective source extent gives the free-field noise.

Step 3: The surface pressure fluctuation is expressed by a model equation in terms of the amplitude and the traversing duration of the impeller blade wake. The free-field characteristics of the noise source are predicted using the modeled pressure fluctuations according to the correlation analysis shown in step 2.

Dipole Strength on the Scroll Surface

Theoretical Background. The relation between the acoustic pressure *Pa* in the free-field and the associated surface pressure fluctuation *Ps* is expressed by Curle's (1955) solution of the Lighthill (1952) equation

$$Pa(x,t) = \frac{1}{4\pi a}\int_S \frac{\cos\theta}{r}\left[\frac{\partial}{\partial t}Ps(y,t)\right]_{\hat{r}} dS(y), \qquad (2)$$

where S denotes the extent of the noise source distributed on

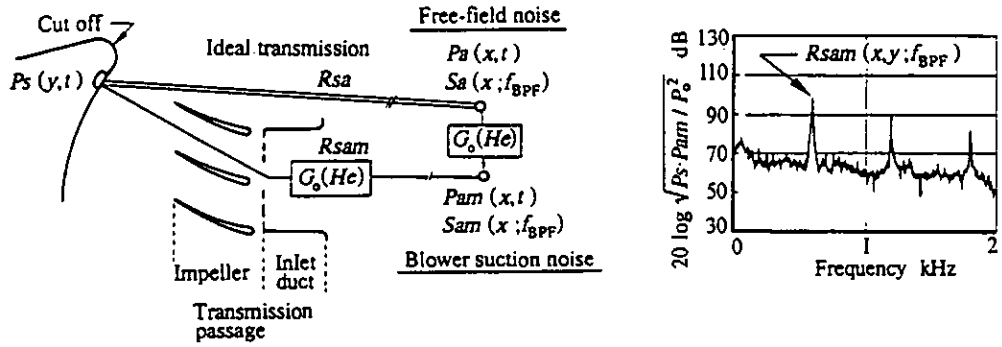

FIG. 5 CORRELATION ANALYSIS FOR EVALUATION OF NOISE SOURCE EXTENT DISTRIBUTED ON THE SCROLL SURFACE.

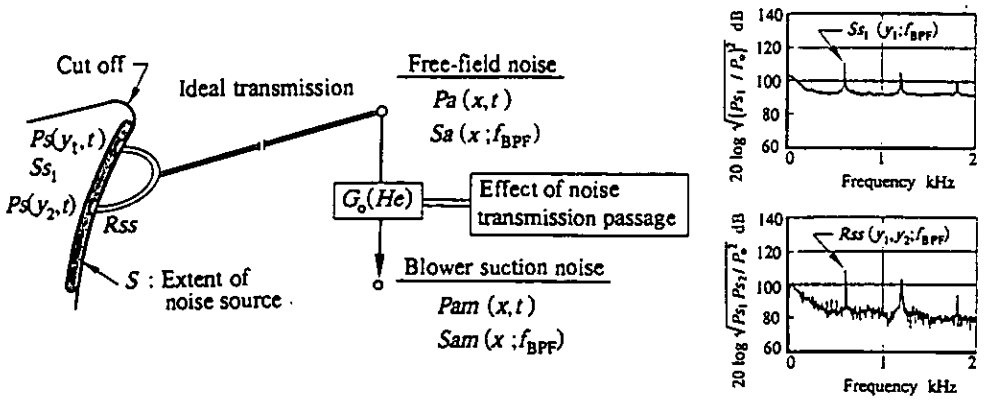

FIG. 6 CORRELATION ANALYSIS FOR BLOWER NOISE PREDICTION.

the scroll surface.

Reflection and diffraction of the sound waves within a casing are ignored since the wavelength of the acoustic pressure is large enough in comparison with blower dimensions. The square brackets [ ] denote evaluation at the retarded time of $\hat{t} = t - r/a$.

Both sides of Eq.(2) are multiplied by the acoustic pressure at a new time $t+\tau$, and by taking a time average,

$$\overline{Pa\,(x,t)\,Pa\,(x,t+\tau)} = \frac{1}{4\pi a} \times \int_S \frac{\cos\theta}{r} \overline{\left[\frac{\partial}{\partial t} Ps\,(y,t)\right]_{\hat{t}} Pa\,(x,t+\tau)}\, dS\,(y)\,. \quad (3)$$

Using the cross-correlation function Csa between Ps and Pa, Eq.(3) may be written as

$$\overline{Pa\,(x,t)\,Pa\,(x,t+\tau)} = -\frac{1}{4\pi a} \times \int_S \frac{\cos\theta}{r} \frac{\partial}{\partial \tau} [Csa]_{\tau + r/a}\, dS\,(y)\,. \quad (4)$$

Two Fourier transforms are introduced as follows:

$$Sa\,(x\,;f) = \int_{-\infty}^{\infty} \overline{Pa\,(x,t)\,Pa\,(x,t+\tau)} \exp(-j\,2\pi f\tau)\, d\tau\,, \quad (5)$$

$$D\,(x,y\,;f\,) = -\frac{\cos\theta}{4\pi a r} \times \int_{-\infty}^{\infty} \frac{\partial}{\partial \tau} [Csa]_{\tau + r/a} \exp(-j\,2\pi f\tau)\, d\tau\,, \quad (6)$$

where Sa is the power spectral density function of the radiated acoustic pressure Pa, and D denotes the surface density spectrum of the noise source, i.e. contribution to the total sound pressure spectrum associated with the unit area of the scroll surface.

In terms of the cross-spectral density function Rsa, the transform D is expressed as

$$D\,(x,y\,;f\,) = -\frac{jf\cos\theta}{2ar} \exp\left(\frac{j2\pi f r}{a}\right) Rsa\,(x,y\,;f)\,. \quad (7)$$

Since the acoustic pressure *Pam* measured at the blower inlet has already influenced by the response characteristics $G_0(He)$ of the noise transmission passage, the functions *Sa* and *Rsa* are expressed as

$$Sa\,(x;f)=Sam\,(x;f)\,/\,G_0\,(f)\ , \tag{8}$$

$$Rsa\,(x,y;f)=Rsam\,(x,y;f)\,/\,\sqrt{G_0(f)}\ , \tag{9}$$

where *Sam* is the power spectral density function of the measured acoustic pressure *Pam*, and *Rsam* denotes the cross-spectral density function between *Ps* and *Pam*.

From Eqs.(7), (8) and (9), we obtain the following relations:

$$Sam\,(x;f)=\int_S D\,(x,y;f)\ \mathrm{d}S\,(y)\ . \tag{10}$$

By means of the precise measurement of *Rsam* at various locations on the scroll surface, distribution of the surface dipole strength, i.e. *D*, is obtained. Then, the complete power spectrum *Sam* is determined by integrating the surface density spectrum *D* over the whole extent of the noise source. Since *Sam* is a real and even function, the imaginary part of *Rsam* tends to zero by the integration, and *Sam* must be doubled to obtain the true power spectrum.

Experimental Results and Discussion. Typical distributions of the surface density spectrum *D* of blade-passing frequency on three kinds of cut off surfaces are indicated in Fig.7. In the measurement, both the magnitude and real part of the complex-valued data of *Rsam* in Eq.(9) are obtained. However, the difference is less than 2 dB, and only the magnitude data of *Rsam* are presented in the figure. The distance *r* appearing in Eq.(7) is determined by the blower geometry as a distance from the scroll surface to the microphone location at the suction side along the passage of the impeller and the duct. Angle θ at the noise source is similarly obtained as an angle between the surface normal and the radiation direction which is assumed to be in the direction of the impeller axis.

The experimental results indicate the following features of the noise source distribution:

(1) In Fig.7(a), the distribution of the surface density spectrum *D* shows an extremely high level in the meridional plane of the impeller and decreases rapidly with the distance η from the rear casing wall. This tendency is unchangeable irrespective of the cut off geometries, and the effective extent of the noise source may be restricted in the vicinity of the impeller meridional plane, as usually accepted. The distribution is largely influenced by the cut off clearance Δr_c, and the level discrepancy between the cases of Δr_c=12 mm and 32 mm is more than 10 dB. However, any significant difference of the radius r_0 of the cut off is not recognized. Therefore, the amplitude discrepancy of the suction noise between the cases of Δr_c=12 mm and 32 mm is caused not by the extent area but by the strength of the noise source.

(2) In the direction ξ along the casing scroll, the surface density spectrum *D* shows the maximum value at the closest point to the impeller on the scroll surface, and gradually decreases to a constant value. The effect of the cut off radius r_0 is proved to be caused only by the extent of the noise source which faces the impeller exit. The difference in the extent is indicated by a shaded area in Fig.7. Two cases of extent of the noise source in the ξ direction are utilized in the integration of Eq.(10); i.e. from the cut off apex to C and D.

The magnitude distribution of the surface density spectrum *D* is represented by 3rd-order spline functions in both η and ξ directions, and integrated over the extent of the noise source according to Eq.(10). The power spectra *Sam* of the suction noise corresponding to two different extents of the noise source are plotted in Fig.11. Both data seem to agree well in the decibel scale with the measured sound pressure level shown

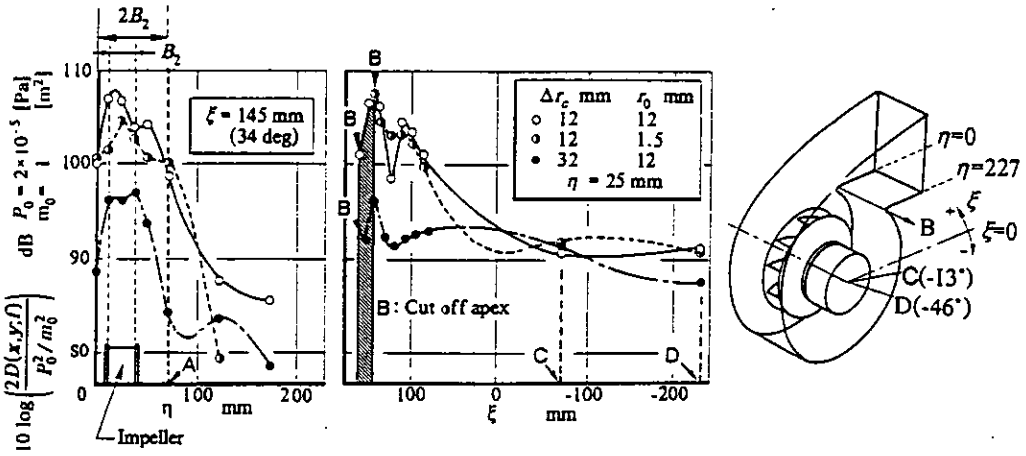

(a) η-DIRECTION (b) ξ-DIRECTION (c) SCROLL COORDINATES

FIG. 7 DISTRIBUTION OF SURFACE DENSITY SPECTRUM ON THE SCROLL SURFACE.

by a thick trace. The two selections of the extent of the noise source do not lead to any significant difference in the results of the integration. The extent of the noise source which contributes to the suction noise essentially lies in the vicinity of the scroll cut off, and the effects of sources located outside of that vicinity are found to be very slight. In the following analyses, the extent of the noise source is assumed to be between the cut off apex and C in the ξ direction, and between the rear casing wall and A, at a distance twice the impeller width, in the η direction.

Characteristics of the Free-Field Noise

Theoretical Background. Since the distance r between the measuring location and the surface source is almost unchanged by the locations of the respective sources, Eq.(2) at a time t may be written as

$$Pa\,(x,t)=\frac{1}{4\pi a r}\int_S \cos\theta\left[\frac{\partial}{\partial t}Ps\,(y,t)\right]_{\hat{t}}\,dS\,(y)\,, \qquad (11)$$

and at a new time of $t+\tau$,

$$Pa\,(x,t+\tau)=\frac{1}{4\pi a r}\int_S \cos\theta\left[\frac{\partial}{\partial t}Ps\,(y,t+\tau)\right]_{\hat{t}}\,dS\,(y)\,. \qquad (12)$$

By taking a product of the respective sides of Eq.(11) and Eq.(12), and taking a time average, the result is

$$\overline{Pa\,(x,t)\,Pa\,(x,t+\tau)}=\left(\frac{1}{4\pi a r}\right)^2 \times\int_S\int_S \cos^2\theta\,\frac{\partial^2}{\partial\tau^2}\left[Css\right]_{\tau+\frac{r_1-r_2}{a}}\,dS\,(y_2)dS\,(y_1)\,, \qquad (13)$$

where Css is the cross-correlation function between the pressure fluctuations measured at locations y_1 and y_2 in the extent of the noise source.

In terms of a cross-spectral density function Rss, a Fourier transform of Eq.(13) is expressed as

$$Sa\,(x;f)=\left(\frac{f}{2a r}\right)^2\int_S\int_S \cos^2\theta\,\exp\left(j2\pi f\,\frac{r_1-r_2}{a}\right) \times Rss\,(y_1,y_2;f)\,dS\,(y_2)\,dS\,(y_1)\,. \qquad (14)$$

The inner-integral of Eq.(14) is replaced by a correlation area Ac_1 which is defined as

$$Ac_1=\int_S \cos^2\theta\,\exp\left(j2\pi f\,\frac{r_1-r_2}{a}\right)\frac{Rss\,(y_1,y_2;f)}{Ss_1(y_1;f)}\,dS\,(y_2)\,, \qquad (15)$$

where normalization of Rss refers to the power spectral density Ss_1 at a source location y_1. The correlation area Ac_1 is the extent area where the pressure fluctuation at location y_1 is effectively converted to a part of the free-field noise, and is evaluated in the present case for the component of the blade-passing frequency. Then, by substituting Eq.(15) for Eq.(14), the power spectral density function Sa of the free-field noise is expressed as

$$Sa\,(x;f)=\left(\frac{f}{2a r}\right)^2\int_S Ac_1\,Ss_1\,(y_1;f)\,dS\,(y_1)\,. \qquad (16)$$

Equation (10) derived in the previous section expresses a simpler formula to relate the suction noise and the surface pressure fluctuation, but it is not suitable for prediction purposes. By knowing the surface pressure fluctuation, Eq.(16) enables us to calculate the free-field noise, and the power spectrum Sam at the blower inlet is immediately obtained by multiplying the frequency-response function $G_0(He)$.

Experimental Results of the Free-Field Noise. The correlation area Ac_1 shown in Eq.(15) is determined by integrating the normalized value of cross-spectral density Rss/Ss_1 which is expressed by the 3rd-order spline function in both η and ξ directions.

The free-field noise level Sa is calculated according to Eq.(16) by integrating the product of the power spectrum of the pressure fluctuation and its correlation area. Third-order spline functions are again used to represent the η- and ξ-directional distribution of the products. The integral is taken over an extent consistent with the extent of the noise source determined in the previous section. The results are plotted by open circles in Fig.11. The data agree well with the presumed free-field noise level indicated by a thin line, which is evaluated by adding the frequency-response function $G_0(He)$ to the measured blower suction noise. The ascending slope is close to 6 and is in accordance with the far-field characteristics of the dipole noise.

Thus, the free-field noise is successfully evaluated from the surface data of the pressure fluctuation applying the correlation analysis. The selection of the extent of the noise source area is found appropriate, and the frequency-response function is proved efficient for noise prediction.

Then, by knowing an expression of the pressure fluctuation on the scroll surface, blower noise prediction becomes possible in terms of the velocity configuration of the impeller discharge. In the following section, characteristics of the discharge velocity and a quasi-steady flow model are presented to describe the pressure fluctuation.

Model of Surface Pressure Fluctuation

Diffusion Characteristics of Blade Wake. The velocity profile of the impeller discharge flow, especially the diffusion characteristics of the blade wake is measured by X hot-film anemometer, since the wake shows large amplitude in the profile of the absolute velocity and is considered to dominate the noise source of the BPF components. The most

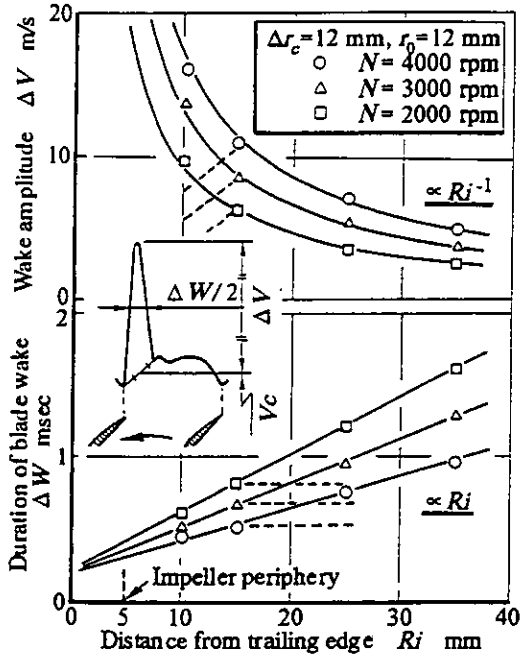

FIG. 8 DIFFUSION CHARACTERISTICS OF BLADE WAKE.

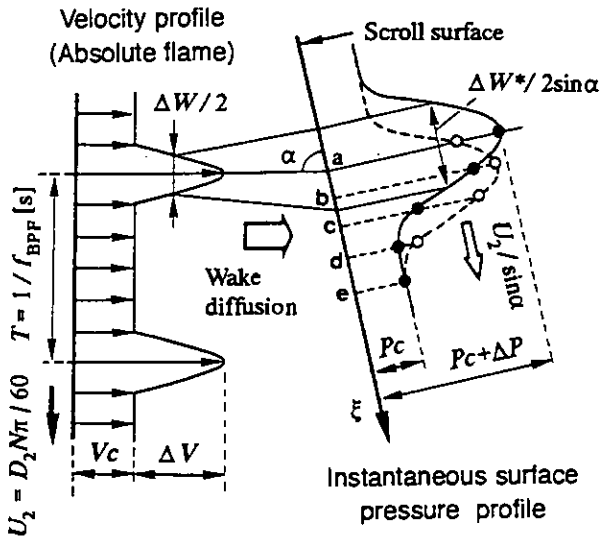

FIG. 9 FLOW MODEL FOR DESCRIBING PRESSURE FLUCTUATIONS ON THE SCROLL SURFACE.

comprehensive parameters to describe the characteristics of wake profile are wake amplitude ΔV and duration of wake ΔW which are defined by Shaw and Balombin (1981) for the absolute velocity of the axial blowers. The definitions of ΔV and ΔW are schematically shown in Fig.8. By changing the distance Ri from the blade trailing edge to the radial direction of the impeller, the characteristics of ΔV and ΔW can be investigated. The results are shown in Fig.8.

Both wake amplitude ΔV and duration of wake ΔW show a simple relationship to the distance Ri from the blade trailing edge, e.g. ΔV and ΔW are proportional to Ri^{-1} and Ri respectively. This relationship is valid for almost every measuring location around the impeller except those locations where the distance between the impeller and the scroll surface is extremely small. In these locations, the wake is suppressed by the scroll surface, and shows the characteristics as represented by the broken lines in Fig.8. However, the discharge velocities from these locations of the impeller impinge on the lower part of the scroll surface where the surface density spectrum of the noise source shows an extremely low level and influences slightly the BPF noise. Thus, the characteristics of the wake diffusion which contributes to the BPF noise are confirmed by the hot-film measurement, and these relations are utilized for the flow model of the surface pressure fluctuations. The utilized data of ΔV and ΔW for the model are measured at the location from where the discharge velocity impinges directly on the extent of the noise source.

Profile of Pressure Fluctuation on the Scroll Surface. In order to have quantitative evaluations of the source strength terms K_D and F_M, a wave model describing the surface pressure fluctuation has been utilized. The outline is schematically shown in Fig.9, and the following assumptions are made:

(1) The velocity profile of the blade wake diffuses between the impeller and the cut off according to the characteristics shown in Fig.8.

(2) The amplitude of the pressure fluctuation on the scroll surface is determined from the instantaneous velocity profile of the impeller blade wake. By assuming a formula of pressure distribution on a jet impinging plate, the fluctuation of the pressure is expressed as (Kamoi and Tanaka, 1977)

$$Ps = \Delta P \exp\left\{-0.694\left(\frac{4\sin\alpha}{\Delta W^*}\xi\right)^2\right\} + Pc \quad , \tag{17}$$

where

$$\Delta P = \frac{1}{2}\rho\left(\Delta V^{*2} + 2Vc^*\Delta V^*\right)\sin^2\alpha \quad , \tag{18}$$

$$Pc = \frac{1}{2}\rho Vc^{*2}\sin^2\alpha \quad . \tag{19}$$

(3) The pressure of such profile travels with the impeller tip speed U_2 along the scroll, and forms the fluctuating pressure wave. The frequency coincides with the blade-passing frequency. The impingement angle α between the wake direction and the scroll tangent of the surface are determined by hot-film velocity measurement.

Thus, the time history of the pressure fluctuation is obtained at an arbitrary point on the scroll surface. A typical waveform of the modeled pressure fluctuation is shown in Fig.10 in comparison with the measured data which was acquired with the scroll mounted microphone. Modeled waveform of the impeller discharge velocity is also indicated in the upper part

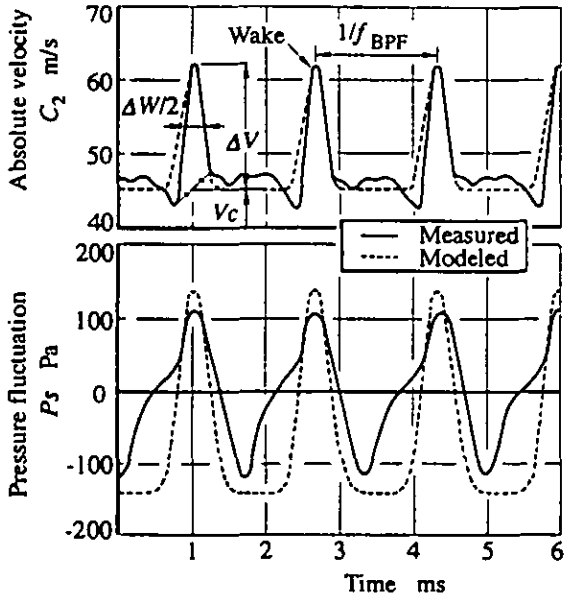

FIG. 10 MODELED WAVEFORMS OF VELOCITY AND PRESSURE FLUCTUATION. COMPARED WITH MEASURED DATA.

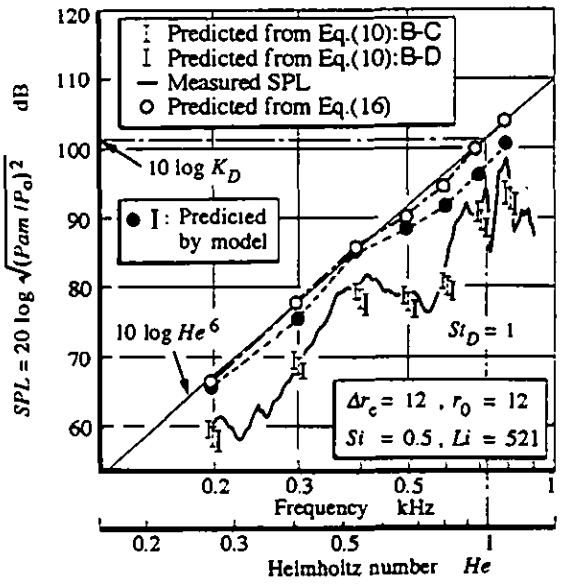

FIG. 11 CHARACTERISTICS OF THE BPF COMPONENTS ESTIMATED BY EXPERIMENTS AND BY A QUASI-STEADY FLOW MODEL.

of the figure. The present model that utilizes the wake parameters ΔV and ΔW to describe the surface pressure fluctuation makes possible an amplitude prediction of the fundamental frequency component.

In the correlation analysis, such time data at five locations are used; i.e. at points a to e in Fig.9. These points correspond to microphone locations in the experiment to evaluate the free-field noise by cross-correlation analysis, and are also located within the assumed noise source extent. In the calculation of the correlation area, uniform distribution of pressure is assumed in span-wise direction η of the scroll surface. Therefore, the correlation area is expressed as a product of length twice the impeller width and the correlation length in the ξ direction which is calculated from integrating the modeled pressure fluctuation. The process of calculating the free-field noise is similar to the process stated before in the experimental evaluation.

Prediction of Blower Suction Noise. The free-field noise calculated by the quasi-steady flow model is shown by the closed circles in Fig.11. The result agrees well with the experimental data indicated by the open circles. The ascending slope in respect to the blower rotational speed is close to 6, which is consistent with the free-field characteristics of the dipole noise. By multiplying the frequency-response function $G_0(He)$, the blower suction noise is obtained as indicated in Fig.11. The noise level predicted by the present model agrees well with the measured BPF trace within a few decibels. Thus, the present model of traveling wake for describing the pressure fluctuations has been satisfactorily utilized in the noise analysis developed in the present research. The assumed extent of the noise source is also proved sufficient for practical use.

The K_D value obtained by applying the quasi-steady flow model is shown for a variation of the cut off clearance Δr_c in Fig.4. For different cases of the clearance, the velocity data of the impeller discharge are determined by measurements. However, the diffusion characteristics of the blade wake are not altered from those shown in Fig.8. Despite the fact that the effect of the cut off radius r_0 could not be taken into account, the predicted value of K_D agrees well with the experimental data. This result indicates that the K_D value is only affected by the amplitude of the surface pressure fluctuation within the noise source extent in the vicinity of the scroll cut off. And the amplitude is mainly caused by the impingement of the impeller blade wake on the scroll surface. The impinging flow of the blade wake is more diffused as the cut off clearance is increased, and then the K_D value decreases. This feature is satisfactorily proved in the figure.

The F_M value expressing the amplitude ratio of the 2nd harmonics to the fundamental BPF noise is also shown in Fig.4. Predicted value of the pressure fluctuation by the present model is seriously low compared with the experimental value. This is an inevitable consequence of the fact that the expression of the pressure fluctuation took account only of the fundamental waveform. As shown in Fig.10, the waveform of the modeled pressure fluctuation does not correspond with that of the measured data except the amplitude level of the fundamental frequency component. In order to have a quantitative evaluation of the F_M value, in other words the r.m.s. level of the higher harmonic components, the effect of other unsteady factors such as vortex shedding and/or scattering pressure waves may be included in the model analysis.

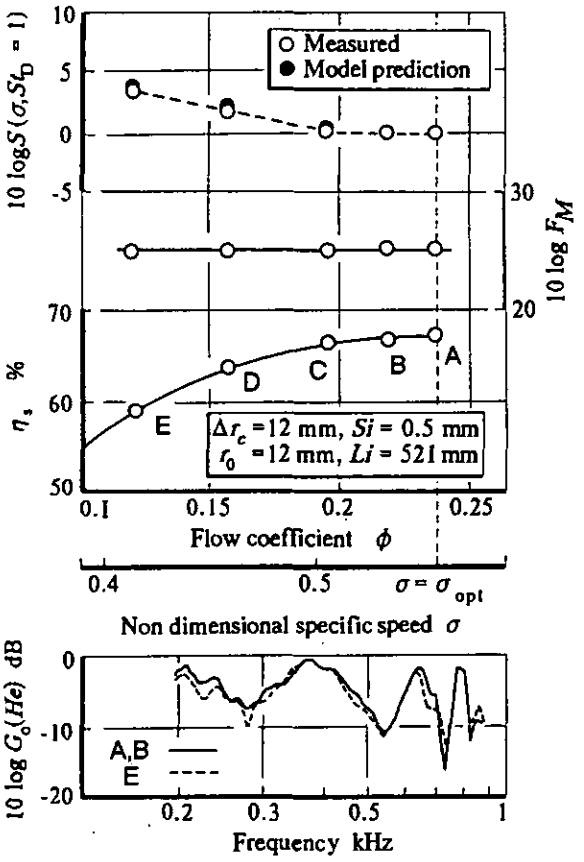

FIG. 12 INFLUENCE OF OFF-DESIGNED OPERATION ON SIMILARITY RULE TERMS.

Influence of Off-Designed Blower Operation. The change in the noise level with a change in the blower flow rate is recognized in previous findings where the noise level increases in accordance with the decrease of flow rate from the maximum-efficiency operation. In the similarity rule shown in Eq.(1), blower flow rate is normalized by introducing a non-dimensional specific speed σ. Since σ is the parameter that only represents the deviation of the operation point, σ constant does not always mean that the blower is operating under maximum-efficiency operation in the case of rotational speed changes. Therefore, in order to confirm the application of the similarity rule to the off-designed operation, the influence of σ on each term of the similarity rule has to be examined. As shown in Fig.12, measurements have been made at 5 points between the maximum and half-flow operation where the broad-band noise level is remarkably low and has no influence nn the BPF components.

Neither the frequency-response function $G_0(He)$ nor the amplitude ratio F_M is influenced by the blower flow rate. The effect only appears at the 1st term of the similarity rule which represents the r.m.s. level of the 1st BPF components. Therefore, the amplitude growth of the blower suction noise in off-designed operation is found to be caused only by the strength of the noise source and not by the response of the transmission passage. The quasi-steady flow model of surface pressure fluctuation presented in the previous section has been utilized in the evaluation of the amplitude growth of the BPF components. The growth is expressed by the correction function S_M in the similarity rule. The results are plotted by closed circles in Fig.12. The present model of surface pressure fluctuation satisfactorily predicts the strength of the noise source between the maximum and half-flow operation. Therefore, taking account of frequency-response function $G_0(He)$ which is unchangeable with the blower flow rate, blower suction noise level even in the off-designed operation can be predicted by utilizing the present model.

CONCLUSIONS

In order to obtain an acoustical and fluid mechanical understanding of centrifugal blower noise, amplitude traces of the blade-passing frequency components versus the blower rotational speed have been discussed by introducing the similarity rule developed by Bommes. The measured data at the blower inlet were decomposed into frequency-response term and source strength terms. Quantitative evaluation of the source strength terms by introducing the correlation analyses and the quasi-steady flow model of surface pressure fluctuation enables us to predict the suction noise level of the blower.

The findings can be summarized as follows:

(1) The extent of the noise source was restricted within the vicinity of the scroll cut off regardless of cut off geometries. The noise reduction in the case of a large cut off clearance was mainly caused by the diffusion of the wake profile. The cut off radius influenced the extent of the noise source.

(2) The free-field noise was determined from the pressure fluctuation data within the extent of the noise source by using cross-correlation analyses. The results agreed well with the experimental data, which were influenced by the frequency-response function described by a one-dimensional wave model. The noise level increased to the 6th power of the impeller rotational speed in accordance with dipole noise characteristics.

(3) The source strength terms of the similarity rule were determined by presenting a quasi-steady flow model of surface pressure fluctuation. In the model, special attention was paid to introduce the diffusion characteristics of the blade wake between the impeller and the scroll surface. The amplitude of the pressure fluctuation was determined by steady-state dynamic pressure of the blade wake. The evaluated data of sound pressure at blower inlet agreed with the experimental data within an uncertainty range of 5 decibels.

(4) The amplitude growth with a change in volume flow rate was satisfactorily evaluated by utilizing the present model between the maximum and half-flow operation.

In the summary, the analysis given here was found to be useful for the purpose of noise predictinn. However, the process of the analysis is very complicated and cumbersome, considerable simplification for practical application would be still necessary. Investigations on the super-harmonics of the BPF noise is further required.

REFERENCES

Akishita, S., Morinushi, K., and Umeda, Y., 1978, "The Surface Dipole Strength Correlated with Vortex Shedding Noise: Experiment on Blunt Trailing-edge Airfoil", *Transactions of the JSME*, Vol.44, No.387, pp.3797-3808, in Japanese.

Bommes, L., 1982, "Analyse und Vorausberechnung des Geräusches von Ventilatoren", *HLH*, Nr.7, pp.245-257.

Curle, N., 1955, "The Influence of Solid Boundaries Upon Aerodynamic Sound", *Proceedings of the Royal Society*, Series A, Vol.231, pp.505-514.

Kamoi, A., and Tanaka H., 1977, "Studies on a Two-Dimensional Impinging Jet Considering Initial Turbulence: 2nd Report, Static Behavior of Boundary Layer in the Stagnation Region", *Transactions of the JSME*, Vol.43, No.372, pp.2957-2973, in Japanese.

Lighthill, M. J., 1952, "On Sound Generated Aerodynamically: General Theory", *Proceedings of the Royal Society*, Series A, Vol.211, pp.564-587.

Maruta, Y., and Kotake, S., 1979a, "Separated-flow Noise of a Flat Plate: 1st Report, Noise Characteristics and Generation Mechanism", *Transactions of the JSME*, Vol.46, No.406, pp.1055-1064, in Japanese.

Maruta, Y., and Kotake, S., 1979b, "Separated-flow Noise of a Flat Plate: 2nd Report, Characteristics of Noise Sources", *Transactions of the JSME*, Vol.46, No.408, pp.1415-1426, in Japanese.

Moreland, J. B., 1974, "Housing Effects on Centrifugal Blower Noise", *Journal of Sound and Vibration*, Vol.36, No.2, pp.191-205.

Neise, W., 1975, "Application of Similarity Laws to the Blade Passage Sound of Centrifugal Fans", *Journal of Sound and Vibration*, Vol.43, No.1, pp.61-75.

Neise, W., 1976, "Noise Reduction in Centrifugal Fans: A Literature Survey", *Journal of Sound and Vibration*, Vol.45, No.3, pp.375-403.

Ohta, Y., Outa, E., and Tajima, K., 1987, "Blade Passing Frequency Noise Induced by Flow around Cut-Off of Scroll in a Centrifugal Fan", *Proceedings of the 1987 Tokyo International Gas Turbine Congress*, Vol.2, pp.231-238.

Ohta, Y., Outa, E., and Tajima, K., 1991, "An Acoustic Model for Prediction of Centrifugal Blower Noise Induced by Blade Discharge Flow around the Scroll Cut Off", *Proceedings of the Yokohama International Gas Turbine Congress*, Vol.2, pp.101-108.

Shaw, L. M., and Balombin, J. R., 1981, "Rotor Wake Characteristics Relevant to Rotor-Stator Interaction Noise Generation", *NASA Technical Memorandum*, Vol.82703, pp.1-24.

Siddon, T. E., 1973, "Surface Dipole Strength by Cross-correlation Method", *Journal of the Acoustical Society of America*, Vol.53, No.2, pp.619-633.

Suzuki, S., and Ugai, Y., 1977, "Study on High Specific Speed Airfoil Fans", *Bulletin of the JSME*, Vol.20, pp.575-582.

Weidemann, J., 1971, "Analysis of the Relations between Acoustic and Aerodynamic Parameters for a Series of Dimensionally Similar Centrifugal Fan Rotors", *NASA Technical Translation*, F-13, pp.1-102.

Yeow, K. W., 1974a, "Acoustic Modeling of Ducted Centrifugal Rotors, (1) The Experimental Acoustic Characteristics of Ducted Centrifugal Rotors", *Journal of Sound and Vibration*, Vol.32, No.1, pp.143-152.

Yeow, K. W., 1974b, "Acoustic Modeling of Ducted Centrifugal Rotors, (2) The Lumped Impedance Model", *Journal of Sound and Vibration*, Vol.32, No.2, pp.203-226.